Report

A multi-stage antimalarial targets the plasmepsins IX and X essential for invasion and egress

Paco Pino[1,*], Reto Caldelari[2], Budhaditya Mukherjee[1], Juha Vahokoski[3], Natacha Klages[1], Bohumil Maco[1], Christine R. Collins[4], Michael J. Blackman[4,5], Inari Kursula[3,6], Volker Heussler[2], Mathieu Brochet[1] and Dominique Soldati-Favre[1,*]

Affiliations:

[1]Department of Microbiology and Molecular Medicine, Faculty of Medicine-University of Geneva CMU, Switzerland.

[2]Institute of Cell Biology, University of Bern; Bern, Switzerland.

[3]Department of Biomedicine, University of Bergen, Jonas Lies vei 91, 5009 Bergen, Norway.

[4]Malaria Biochemistry Laboratory, The Francis Crick Institute, Mill Hill, London NW1 1AT, UK.

[5]Department of Pathogen Molecular Biology, London School of Hygiene & Tropical Medicine, London WC1E 7HT, UK

[6]Biocenter Oulu & Faculty of Biochemistry and Molecular Medicine, University of Oulu, Aapistie 7, 90220 Oulu, Finland.

*Corresponding authors: Paco.Pino@unige.ch, Dominique.Soldati-favre@unige.ch

Keywords:

Malaria, *Plasmodium falciparum, Plasmodium berghei,* aspartic protease, invasion, egress, exflagellation, transmission, hydroxyl-ethyl-amine scaffold, peptidomimetic inhibitor, protein maturase.

Abstract

Regulated exocytosis by secretory organelles is important for malaria parasite invasion and egress. Many parasite effector proteins, including perforins, adhesins, and proteases, are extensively proteolytically processed both pre- and post-exocytosis. Here, we report the multi-stage anti-plasmodial activity of the aspartic protease inhibitor hydroxyl-ethyl-amine-based scaffold compound, 49c. This scaffold inhibits the pre-exocytosis processing of several secreted rhoptry and microneme proteins by targeting the corresponding maturases plasmepsins IX (PfPMIX) and X (PfPMX), respectively. Conditional excision of PfPMIX revealed its crucial role in invasion, and recombinantly active PfPMIX and PfPMX cleave egress and invasion factors in a 49c sensitive manner.

One Sentence Summary: An aspartic protease inhibitor targeting plasmepsins IX and X acts as an antiplasmodial compound blocking infection and transmission at subnanomolar concentrations.

Main Text

Malaria remains a major cause of mortality worldwide, and resistance to existing antimalarials is a growing problem, that requires the development of new drugs urgently. Aspartic proteases are potential targets for chemotherapy (*1*), and key contributors to *Plasmodium falciparum* pathogenicity (*2, 3*). *P. falciparum* possesses a repertoire of 10 aspartic proteases, named plasmepsins (PMI to X). PMIX and PMX are expressed in mature blood-stage schizonts and invasive merozoites and fulfill indispensable but unknown functions. The activity of several serine and cysteine proteases promotes the destabilization of the parasitophorous vacuole membrane (PVM) and red blood cell (RBC) membranes which surround the parasite (*4*). Egress is followed by invasion of a fresh RBC, a process that takes 10-30 s. Invasion also crucially relies on serine proteases to activate or remove ligands involved in interactions with the host erythrocyte (*5*).

To study the role of aspartic proteases during egress and invasion, we used a hydroxyl-ethyl-amine scaffold that inhibits aspartic proteases by mimicking the tetrahedral intermediate of hydrolysis (*6*). Compound 49c **(Fig. 1A)** is such a peptidomimetic competitive inhibitor and has been found to be effective against *P. falciparum in vitro* and the rodent parasite *Plasmodium berghei in vivo* (*7, 8*). This compound has a modest effect after 24 hours treatment (IC_{50} > 500 nM) and a significantly greater effect after 72 hours (IC_{50} 0.6 nM), indicating inhibition occurs at a specific life-cycle stage. *P. falciparum* cultures treated at ring stage with 1 nM 49c showed no difference compared to controls during the first 24 hours, contrasting with a total disappearance of the parasites after three days (**Fig. 1B**). The killing profile of 49c is comparable to chloroquine (CQ), with a 99.9% parasite clearance (*9*) achieved at 48 hours of treatment (**Fig. 1C**). Importantly, 49c did not affect intraerythrocytic development and allowed the production of microscopically normal schizonts that were, however, not released from the host cell (**Fig. 1D).** Treatment 5 hours prior to egress was

sufficient to inhibit egress, whereas treatment for 3 hours had no significant effect **(Fig. 1E**). Removal of 49c 1 hour prior to egress did not release the block, whereas washing it out 5 hours before egress totally rescued the phenotype (**Fig. 1F**), confirming that 49c acts during late schizogony to block egress but does not prevent intra-erythrocytic development.

Plasmodium egress from infected red blood cells (iRBCs) is a two-step process, initiated by the disruption of the PVM followed by the erythrocyte membrane. These two steps require the serine protease PfSUB1 (*10, 11*), which undergoes at least two proteolytic processing events during its maturation to produce the mature p47 form (**Fig. 1G**) (*12*). Treatment of parasites with 10 nM 49c prevented the p54-to-p47 transition, while 1 nM 49c resulted in traces of mature p47 PfSUB1 (**Fig. 1G-H**). 49c had no impact on the trafficking and secretion of PfSUB1 from exonemes as no difference was observed comparing 49c-treated and control egressing schizonts (**Fig. S1A**) and did not inhibit the enzymatic activity of recombinant PfSUB1 *in vitro* (**Fig. S1B**). PfSUB1 governs egress by processing the merozoite surface protein PfMSP1 (*11*) and SERA family proteins in the PV (**Fig. S1I**) (*13*). Both PfMSP1 and PfSERA5 remained unprocessed in parasites treated with 49c, indicating that PfSUB1 was inactive (**Fig. S1C-E**). We visualized the effect of 49c on PVM breakdown, using parasites expressing a GFP fusion of the soluble PV protein PfPVI (PfPVI-GFP) (*14*). When the PVM ruptures, pores form in the iRBC membrane, leading to the disappearance of the GFP signal (*15*). In control parasites, the extremely short period between PVM rupture and egress could not be observed. In contrast, parasites treated with 1 nM 49c were able to break the PVM but remained trapped within the RBCs, while 10 nM 49c completely blocked PVM rupture (**Fig. S1F**). These results were confirmed by transmission electron microscopy (EM) (**Fig. 1I**).

We assessed the impact of 49c on erythrocyte invasion by mechanically releasing merozoites (*16*). Treatment with 49c >5 hours impaired invasion, whereas a 1-hour treatment had no significant impact (**Fig. 1J**). Invasion critically relies on the formation of a moving junction

composed of the apical membrane antigen-1 (PfAMA1) and rhoptry proteins (PfRONs) (*17*). PfAMA1 (*18*) is a microneme, integral membrane protein, which is processed by the action of an unknown protease at its N-terminus to generate the secreted p66 form from a p83 precursor (**Fig. S1G)**. This event occurs prior to exocytosis and appears to be a prerequisite for PfAMA1 secretion (*19*). Consistently, 49c abrogated the processing of PfAMA1, resulting in accumulation of the p83 precursor (**Fig. 1K**) without impacting PfAMA1 trafficking to the micronemes (**Fig. S1H).**

Within erythrocytic stages, PMIX and PMX are predominantly expressed at the schizont stage, suggesting a role in egress and/or invasion and implicating them as plausible targets for 49c (**Fig. S2A)** (*20*). *PMIX* and *PMX* appeared to be refractory to genetic ablation in both *P. falciparum* and *P. berghei (21)*. We therefore opted for conditional expression systems, DiCre (*22*) for PfPMIX and the auxin-inducible degron approach (*23*) for PbPMIX and PbPMX. The *P. berghei* inducible knockdowns showed only low levels of protein destabilization (**Fig. S3A-B**). We modified the *PfPMIX* locus to insert loxP sites and a C-terminal epitope tag in DiCre expressing parasites (*22*) (**Fig. S4A-B**). PfPMIX-Ty only partially co-localised with PfCyRPA and PfRhopH3 but not with PfAMA1 (**Fig. 2A**). The localization at the proximity of the rhoptries was confirmed by immune electron microscopy (**Fig. S4C-D**) and is concordant with transcriptomes information from indicating expression prior to secretory organelle proteins (*24*). Induction of DiCre activity by rapamycin led to the complete disappearance of PfPMIX (**Fig. 2B**). PfPMIX-deficient parasites became undetectable three days after rapamycin treatment (**Fig. 2C**). In the absence of PfPMIX, intracellular development occurred normally until the schizont stage (**Fig. 2D**). Consistent with its expression in schizonts (**Fig. S2A**), ring-stage parasites were significantly reduced by the second cycle after rapamycin treatment showing a severe default in invasion. This decline in erythrocyte invasion was more pronounced when the samples were treated with trypsin to

remove non-invasive adherent merozoites from the host cell surface (**Fig. 2E**). Any delay in the egress process results in non-invasive merozoites, probably due to the exhaustion of their secreted protein set (*16*). The replication defect in parasites lacking PfPMIX did not result from impaired egress (*25*), as time-lapse video-microscopy (*11*) did not reveal delayed egress (**Fig. S4C** and **Movies S1** and **S2**), confirming that PfPMIX is essential for invasion only.

We identified the rhoptry associated protein 1 (PfRAP1) and the apical sushi protein (PfASP) as substrates of PfPMIX. Both proteins are targeted to the rhoptry and are extensively processed during their maturation (*26, 27*). PfRAP1 is converted from a short-lived, 86-kDa precursor into an 82 kDa (p82) form which is then converted to a 67 kDa (p67) form during schizont maturation (*28*). Importantly, the p86 precursor accumulated in the absence of PfPMIX, as well as upon treatment with 100 nM and 1 μM 49c, suggesting that 49c targets PfPMIX (**Fig. 2 F)** but apparently less potently than the protease responsible for PfSUB1 activation (**Fig. 1 F**). PfASP processing was also impaired in PfPMIX-KD parasites and a 1nM treatment 49c resulted in similar inhibition (**Fig. 2G**). A difference in 49c activity against various substrates of PfPMIX is not unexpected as 49c acts as a peptidomimetic competitive inhibitor (*6*).

To ensure that both rhoptry proteins represent direct substrates of PfPMIX, we expressed recombinant active (rPfPMIX, rPfPMX) as well as the catalytically dead mutants (rPfPMIX D/A, rPfPMX D/A) in baculovirus-infected insect cells. Both rPfPMIX and rPfPMX were active against the *Toxoplasma gondii* ROP1 peptide (*29*) and sensitive to 49c (**Fig. S5A-D**). Remarkably, rPfPMIX but not rPfPMIX D/A or rPfPMX showed activity on PfRAP-derived peptide but not on a mutant peptide and was inhibited by 1 μM 49c (**Fig. 2H**). Concordantly rPfPMIX was active against PfRAP1 immunoprecipitated from PfPMIX-KD parasites (**Fig. S6A**). Similarly, PfASP purified from PfPMIX-KD parasite supernatant was efficiently processed by rPfPMIX but not when 1μM 49c was added to the assay or with rPfPMX D/A

or rPfPMX (**Fig. S6B**).

The reticulocyte-binding homolog 5 (PfRh5) binds to erythrocyte basigin and is essential for merozoite invasion (*30*) and acts in concert with PfRipr and PfCyRPA (*31*) as well as Pfp113 (*32*). While PfRh5, PfRipr and Pfp113 are processed and released normally in the absence of PfPMIX, very little PfCyRPA is detectable in the supernatant during egress (**Fig. S6C-E)**. CyRPA is not known to be processed, and the defect observed in PfCyRPA release remains unexplained but might contribute to loss of invasiveness in the absence of PfPMIX.

Since PfAMA1, PfSUB1, PfSERA5, and PfMSP1 are processed normally in the absence of PfPMIX but not upon 49c treatment (**Fig. S6C-E**), we hypothesized that PfPMX is responsible for the maturation of PfAMA1 and PfSUB1, We were, however, unable to conditionally knock-down PfPMX expression in either *P. falciparum* or *P. berghei* (**Fig. S3A, B**). Instead, we show that rPfPMX cleaves *in vitro* fluorogenic peptides corresponding to the PfAMA1 p83-to-p66 (*33*) (**Fig. 2I)** and to PfSUB1 p54-to-p47 cleavage sites (**Fig. 2J),** as well as the recombinant PvSUB1 **(Fig. S6F**). Importantly, 49c inhibited rPfPMX activity *in vitro* validating PfAMA1 and PfSUB1 as substrates for PfPMX. Decisively 49c dually targets PfPMIX and PfPMX and hence provides a rationale for the failure to isolate resistant parasites (**Fig. S6H**).

The antiplasmodial activity of 49c *in vivo* was characterized using the rodent model *P. berghei*. Based on the pharmacokinetics of 49c in mice (**Fig. S7A**), we opted for intraperitoneal (ip) injection of 100 mg/kg 49c that sustained blood concentrations higher than 0.2 µM over a 24 hours window. Daily treatment for 4 days cleared parasites from peripheral blood (**Fig. 3A and B**). Following initial treatment, circulating schizonts accumulated in the blood, confirming that 49c also blocked *P. berghei* egress from RBCs (**Fig. 3C and Fig. S7B**). No parasites were detectable after 2 weeks of treatment.

Transmission is mediated by an obligatory sexual life cycle phase (**Fig. S7D**), and drugs

blocking transmission to the mosquito vector are potentially valuable for malaria eradication. Although 49c did not affect differentiation from asexual stages into microscopically mature gametocytes (**Fig. 3C**), it prevented further development into fertile gametes. Upon mosquito ingestion, each male gametocyte differentiates into eight sperm-like microgametes that are released in a process termed exflagellation. A 48-hour treatment with 49c led to a 10-fold decrease in exflagellation (**Fig. 3D**) and prevented the lysis of the RBC membranes surrounding both male and female parasites (**Fig. 3E**). Both PbPMX and its substrate PbSUB1 are expressed in mature gametocytes while PbPMIX could not be detected in these stages (**Fig. 3F and G**). Consistently, a 48-hour treatment with 49c strongly reduced PbSUB1 processing pointing to a conserved proteolytic cascade required for the egress of both asexual and sexual erythrocytic stages. Treatment at the time of gametogenesis activation had no effect on exflagellation, indicating that PMX activity is required for parasite egress during gametocytogenesis prior to mosquito ingestion (**Fig. 3H**).

Egress of gametes from the host erythrocyte is followed by fertilization. Within 24 hours, zygotes transform into ookinetes, which colonize the epithelial monolayer of the mosquito midgut. 49c treatment during *in vivo* gametocytogenesis completely blocked ookinete formation (**Fig. 3I**). Conversely, treatment at the onset of gametogenesis did not prevent the development of ookinetes (**Fig. 3J**). We were not able to detect PbSUB1 in ookinetes but 49c inhibited processing of the micronemal protein PbCelTOS that occurs during the late stages of ookinete development (**Fig. 3K**). PbCelTOS is crucial for ookinetes to traverse host cells into the site of oocyst development (*34*). Similar to gametocytes, PbPMX but not PbPMIX was detected in ookinetes (**Fig. 3F**) and, *in vitro* assays revealed that rPfPMX cleaved immunoprecipitated PbCelTOS-HA (**Fig. 3L**). In light of the potent inhibitory effect of 49c on gametogenesis and ookinete biology, we assessed the transmission blocking potential of

49c *in vivo*. A single treatment of infected mice 30 hours before blood meal completely blocked oocyst formation in the midgut of *Anopheles* mosquitoes (**Fig. 3M and N**).

Several studies have highlighted the commonalities between the blood and hepatic stages with regard to egress and invasion strategies as illustrated for SUB1 (*13, 35, 36*) and AMA1 (*37*), respectively. The effects of 49c on hepatic stage development with the focus on egress of *P. berghei* were examined using HeLa as well as HepG2 cells infected with mCherry-expressing *P. berghei* sporozoites. 49c added 2 hours post infection neither affected the number of infected cells (**Fig. S8A, E and F**) nor the size of intrahepatic parasites *in vitro* after 48 hours (**Fig. S8B G and H**). Infected cells detach upon rupture of the PVM, which typically occurs between 55 and 60 hours post infection (*38*). 49c led to a dramatic reduction of detached cells at doses as low as 6 nM, and no detached cells at all in the presence of 25 nM 49c (**Fig. 4A and S8C-D**). Merozoite development was normal, but progression to detached cells was hampered, resulting in accumulation of merozoite stage parasites at the time of cell detachment (**Fig. 4B**). Staining with MSP1, a marker for successful liver stage development, confirmed that 49c does not affect merozoite development (**Fig. 4B** and **4C)**. An *in vivo* time-course experiment was conducted with mice infected with luciferase-expressing *P. berghei* sporozoites and either treated twice with 100 mg/kg 49c, or left untreated (**Fig 4D**). The livers of drug-treated and control infected mice were comparably infected at 44 hours post infection, as revealed by bioluminescence imaging. Control mice exhibited the typical disappearance of signal from the liver after 55 hours and the concomitant appearance in blood after 65 hours (**Fig. 4E**). The liver load was prolonged in the presence of 49c, likely due to impaired egress, and blood stage development was strongly delayed, as analyzed by FACS in the blood of infected animals (**Fig. 4F**). 49c treatment had a strong effect on the establishment of blood stage parasites, although, at the administered doses, a complete block was not achieved.

Curative and preventive strategies for malaria treatment should ideally target three malarial life cycle stages: exoerythrocytic forms, the asexual blood stages, and the transmission stages. Here, we show that the pleiotropic plasmepsin inhibitor 49c inhibits malarial PMIX and PMX, resulting in a block in blood stage parasite egress and invasion as well as hepatic stage egress and transmission. Taken together PMIX and PMX qualify as very promising dual targets toward malaria eradication.

References and Notes:

1. B. E. Sleebs *et al.*, Transition state mimetics of the *Plasmodium* export element are potent inhibitors of plasmepsin V from *P. falciparum* and *P. vivax*. *Journal of medicinal chemistry*, (2014).
2. J. A. Boddey *et al.*, An aspartyl protease directs malaria effector proteins to the host cell. *Nature* **463**, 627-631 (2010).
3. I. Russo *et al.*, Plasmepsin V licenses *Plasmodium* proteins for export into the host erythrocyte. *Nature* **463**, 632-636 (2010).
4. C. R. Collins *et al.*, The *Plasmodium falciparum* pseudoprotease SERA5 regulates the kinetics and efficiency of malaria parasite egress from host erythrocytes. *PLoS Pathog* **13**, e1006453 (2017).
5. G. E. Weiss *et al.*, Overlaying Molecular and Temporal Aspects of Malaria Parasite Invasion. *Trends in parasitology* **32**, 284-295 (2016).
6. R. Recacha *et al.*, Structures of plasmepsin II from *Plasmodium falciparum* in complex with two hydroxyethylamine-based inhibitors. *Acta Crystallogr F Struct Biol Commun* **71**, 1531-1539 (2015).
7. C. L. Ciana *et al.*, Novel in vivo active anti-malarials based on a hydroxy-ethyl-amine scaffold. *Bioorganic & medicinal chemistry letters* **23**, 658-662 (2013).

8. W. A. Guiguemde *et al.*, Chemical genetics of *Plasmodium falciparum*. *Nature* **465**, 311-315 (2010).

9. L. M. Sanz *et al.*, *P. falciparum* in vitro killing rates allow to discriminate between different antimalarial mode-of-action. *PloS one* **7**, e30949 (2012).

10. S. Glushakova *et al.*, Irreversible effect of cysteine protease inhibitors on the release of malaria parasites from infected erythrocytes. *Cellular microbiology* **11**, 95-105 (2009).

11. S. Das *et al.*, Processing of *Plasmodium falciparum* Merozoite Surface Protein MSP1 Activates a Spectrin-Binding Function Enabling Parasite Egress from RBCs. *Cell host & microbe* **18**, 433-444 (2015).

12. M. Sajid *et al.*, Maturation and specificity of *Plasmodium falciparum* subtilisin-like protease-1, a malaria merozoite subtilisin-like serine protease. *The Journal of biological chemistry* **275**, 631-641 (2000).

13. S. Yeoh *et al.*, Subcellular discharge of a serine protease mediates release of invasive malaria parasites from host erythrocytes. *Cell* **131**, 1072-1083 (2007).

14. T. Chu *et al.*, Genetic evidence strongly support an essential role for PfPV1 in intra-erythrocytic growth of *P. falciparum*. *PloS one* **6**, e18396 (2011).

15. S. Glushakova *et al.*, New stages in the program of malaria parasite egress imaged in normal and sickle erythrocytes. *Curr Biol* **20**, 1117-1121 (2010).

16. M. J. Boyle *et al.*, Isolation of viable *Plasmodium falciparum* merozoites to define erythrocyte invasion events and advance vaccine and drug development. *Proceedings of the National Academy of Sciences of the United States of America* **107**, 14378-14383 (2010).

17. M. H. Lamarque *et al.*, Plasticity and redundancy among AMA-RON pairs ensure host cell entry of *Toxoplasma* parasites. *Nat Commun* **5**, 4098 (2014).

18. A. Yap *et al.*, Conditional expression of apical membrane antigen 1 in *Plasmodium falciparum* shows it is required for erythrocyte invasion by merozoites. *Cellular microbiology* **16**, 642-656 (2014).

19. J. Healer *et al.*, Functional analysis of *Plasmodium falciparum* apical membrane antigen 1 utilizing interspecies domains. *Infect Immun* **73**, 2444-2451 (2005).

20. R. Banerjee *et al.*, Food vacuole plasmepsins are processed at a conserved site by an acidic convertase activity in *Plasmodium falciparum*. *Molecular and biochemical parasitology* **129**, 157-165 (2003).

21. C. Pfander *et al.*, A scalable pipeline for highly effective genetic modification of a malaria parasite. *Nat Methods* **8**, 1078-1082 (2011).

22. C. R. Collins *et al.*, Robust inducible Cre recombinase activity in the human malaria parasite *Plasmodium falciparum* enables efficient gene deletion within a single asexual erythrocytic growth cycle. *Molecular microbiology* **88**, 687-701 (2013).

23. N. Philip *et al.*, Conditional Degradation of *Plasmodium* Calcineurin Reveals Functions in Parasite Colonization of both Host and Vector. *Cell host & microbe* **18**, 122-131 (2015).

24. Z. Bozdech *et al.*, The transcriptome of the intraerythrocytic developmental cycle of *Plasmodium falciparum*. *PLoS biology* **1**, E5 (2003).

25. A. Mbengue *et al.*, Novel *Plasmodium falciparum* Maurer's clefts protein families implicated in the release of infectious merozoites. *Molecular microbiology* **88**, 425-442 (2013).

26. D. L. Baldi *et al.*, Identification and disruption of the gene encoding the third member of the low-molecular-mass rhoptry complex in *Plasmodium falciparum*. *Infect Immun* **70**, 5236-5245 (2002).

27. A. H. O'Keeffe *et al.*, A novel Sushi domain-containing protein of *Plasmodium falciparum*. *Molecular and biochemical parasitology* **140**, 61-68 (2005).

28. R. F. Howard *et al.*, Analysis of the processing of *Plasmodium falciparum* rhoptry-associated protein 1 and localization of Pr86 to schizont rhoptries and p67 to free merozoites. *Molecular and biochemical parasitology* **92**, 111-122 (1998).

29. D. Soldati *et al.*, Processing of *Toxoplasma* ROP1 protein in nascent rhoptries. *Molecular and biochemical parasitology* **96**, 37-48 (1998).

30. C. Crosnier *et al.*, Basigin is a receptor essential for erythrocyte invasion by *Plasmodium falciparum*. *Nature* **480**, 534-537 (2011).

31. J. C. Volz *et al.*, Essential Role of the PfRh5/PfRipr/CyRPA Complex during *Plasmodium falciparum* Invasion of Erythrocytes. *Cell host & microbe* **20**, 60-71 (2016).

32. F. Galaway *et al.*, P113 is a merozoite surface protein that binds the N terminus of *Plasmodium falciparum* RH5. *Nat Commun* **8**, 14333 (2017).

33. S. A. Howell *et al.*, Proteolytic processing and primary structure of *Plasmodium falciparum* apical membrane antigen-1. *The Journal of biological chemistry* **276**, 31311-31320 (2001).

34. T. Kariu *et al.*, CelTOS, a novel malarial protein that mediates transmission to mosquito and vertebrate hosts. *Molecular microbiology* **59**, 1369-1379 (2006).

35. C. Suarez *et al.*, The malarial serine protease SUB1 plays an essential role in parasite liver stage development. *PLoS Pathog* **9**, e1003811 (2013).

36. L. Tawk *et al.*, A key role for *Plasmodium* subtilisin-like SUB1 protease in egress of malaria parasites from host hepatocytes. *The Journal of biological chemistry* **288**, 33336-33346 (2013).

37. O. Silvie *et al.*, A role for apical membrane antigen 1 during invasion of hepatocytes by *Plasmodium falciparum* sporozoites. *The Journal of biological chemistry* **279**, 9490-9496 (2004).

38. A. Sturm *et al.*, Manipulation of host hepatocytes by the malaria parasite for delivery into liver sinusoids. *Science* **313**, 1287-1290 (2006).

39. M. A. Child *et al.*, Regulated maturation of malaria merozoite surface protein-1 is essential for parasite growth. *Molecular microbiology* **78**, 187-202 (2010).

40. R. Stallmach *et al.*, *Plasmodium falciparum* SERA5 plays a non-enzymatic role in the malarial asexual blood-stage lifecycle. *Molecular microbiology* **96**, 368-387 (2015).

41. C. Crosnier *et al.*, A library of functional recombinant cell-surface and secreted *P. falciparum* merozoite proteins. *Mol Cell Proteomics* **12**, 3976-3986 (2013).

42. M. L. Tonkin *et al.*, Host cell invasion by apicomplexan parasites: insights from the co-structure of AMA1 with a RON2 peptide. *Science* **333**, 463-467 (2011).

43. K. S. Reddy *et al.*, Multiprotein complex between the GPI-anchored CyRPA with PfRH5 and PfRipr is crucial for *Plasmodium falciparum* erythrocyte invasion. *Proceedings of the National Academy of Sciences of the United States of America* **112**, 1179-1184 (2015).

44. P. Pino *et al.*, A tetracycline-repressible transactivator system to study essential genes in malaria parasites. *Cell host & microbe* **12**, 824-834 (2012).

45. F. Plattner *et al.*, *Toxoplasma* profilin is essential for host cell invasion and TLR11-dependent induction of an interleukin-12 response. *Cell host & microbe* **3**, 77-87 (2008).

46. G. Rugarabamu *et al.*, Distinct contribution of *Toxoplasma gondii* rhomboid proteases 4 and 5 to micronemal protein protease 1 activity during invasion. *Molecular microbiology* **97**, 244-262 (2015).

47. C. Lambros *et al.*, Synchronization of *Plasmodium falciparum* erythrocytic stages in culture. *J Parasitol* **65**, 418-420 (1979).

48. P. K. Harris *et al.*, Molecular identification of a malaria merozoite surface sheddase. *PLoS Pathog* **1**, 241-251 (2005).

49. J. A. Thomas *et al.*, Development and Application of a Simple Plaque Assay for the Human Malaria Parasite *Plasmodium falciparum*. *PloS one* **11**, e0157873 (2016).

50. C. R. Collins *et al.*, Malaria parasite cGMP-dependent protein kinase regulates blood stage merozoite secretory organelle discharge and egress. *PLoS Pathog* **9**, e1003344 (2013).

51. C. Withers-Martinez *et al.*, *Plasmodium* subtilisin-like protease 1 (SUB1): insights into the active-site structure, specificity and function of a pan-malaria drug target. *International journal for parasitology* **42**, 597-612 (2012).

52. M. J. Blackman *et al.*, Structural and biochemical characterization of a fluorogenic rhodamine-labeled malarial protease substrate. *Biochemistry* **41**, 12244-12252 (2002).

53. C. Withers-Martinez *et al.*, The malaria parasite egress protease SUB1 is a calcium-dependent redox switch subtilisin. *Nat Commun* **5**, 3726 (2014).

54. D. J. Fitzgerald *et al.*, Protein complex expression by using multigene baculoviral vectors. *Nat Methods* **3**, 1021-1032 (2006).

55. M. Buchs *et al.*, High-throughput insect cell protein expression applications. *Methods in molecular biology* **498**, 199-227 (2009).

56. M. J. Coffey *et al.*, An aspartyl protease defines a novel pathway for export of *Toxoplasma* proteins into the host cell. *Elife* **4**, (2015).

57. D. W. Wilson *et al.*, Macrolides rapidly inhibit red blood cell invasion by the human malaria parasite, *Plasmodium falciparum*. *BMC Biol* **13**, 52 (2015).

58. D. T. Riglar *et al.*, Super-resolution dissection of coordinated events during malaria parasite invasion of the human erythrocyte. *Cell host & microbe* **9**, 9-20 (2011).

59. L. Chen *et al.*, An EGF-like protein forms a complex with PfRh5 and is required for invasion of human erythrocytes by *Plasmodium falciparum*. *PLoS Pathog* **7**, e1002199 (2011).

60. G. R. Mair *et al.*, Universal features of post-transcriptional gene regulation are critical for *Plasmodium* zygote development. *PLoS Pathog* **6**, e1000767 (2010).

61. M. Brochet *et al.*, Phosphoinositide metabolism links cGMP-dependent protein kinase G to essential Ca(2)(+) signals at key decision points in the life cycle of malaria parasites. *PLoS biology* **12**, e1001806 (2014).

62. P. C. Burda *et al.*, A *Plasmodium* phospholipase is involved in disruption of the liver stage parasitophorous vacuole membrane. *PLoS Pathog* **11**, e1004760 (2015).

63. M. De Niz *et al.*, The machinery underlying malaria parasite virulence is conserved between rodent and human malaria parasites. *Nat Commun* **7**, 11659 (2016).

Acknowledgments:

We are grateful to Dr. C. Boss (Actelion Pharmaceuticals Ltd) and Dr. S. Wittlin for providing us the initial 49c stock and for their help with the chemical synthesis. We thank Dr. G. Wright, Dr. M. Lebrun, Dr. D. Gaur and Dr. A. Cowman for the gift of numerous antibodies. We are grateful to Dr. O. Billker for the gift of Compound 2, and F. Hackett, J. B. Marq, and Ju Xu for their technical assistance. We thank the excellent service at the Biocenter Oulu Mass Spectrometry Core Facility. We would like to thank the PlasmoGEM team (Wellcome Trust Sanger Institute) for providing the PlasmoGEM vectors. We would like to thank the Netherlands Cancer Institute (NKI) Protein Facility for provision of the LIC

vector and the Nederlandse Organisatie voor Wetenschappelijk Onderzoek (NWO) for financial support to the facility (grant nr. 175.010.2007.012).

This work was funded by Carigest SA (DSF), the Swiss National Foundation (Grant 156825 to PP, 310030B_166678 to DSF, 310030_159519 to VH and BSSGI0_155852 to MB), SystemsX.ch (51TRPO_151032, VH and DSF), and the Academy of Finland (257537 and 292718 to IK). Funding to MJB was from the Francis Crick Institute (https://www.crick.ac.uk/) and Wellcome ISSF2 funding to the London School of Hygiene & Tropical Medicine.

Figure 1

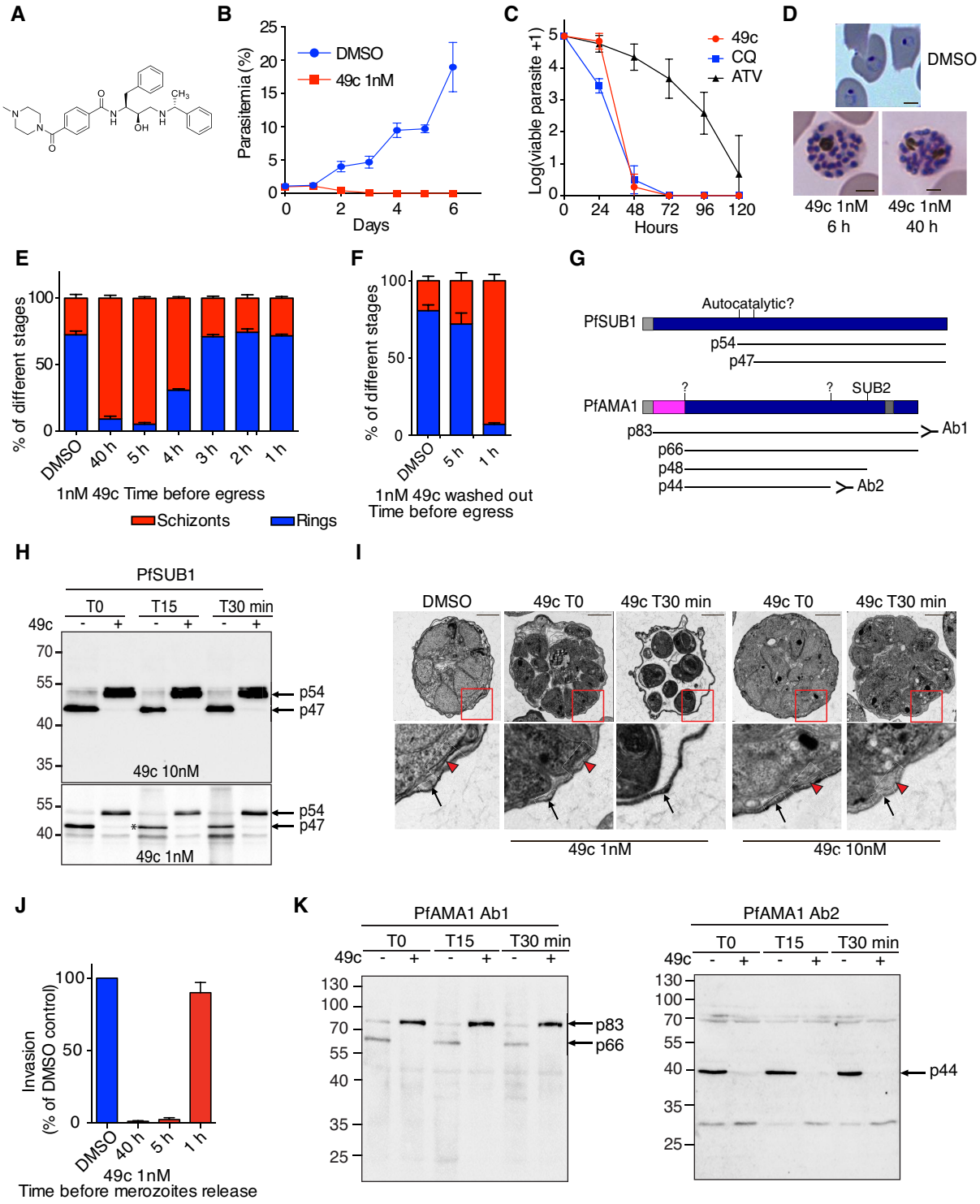

Figure 1. Compound 49c prevents *Plasmodium falciparum* merozoite egress and invasion.

A) Structure of compound 49c. **B)** WT *P. falciparum* parasites were treated with 1nM 49c or DMSO, and parasitemia was quantified daily over a six day a period by counting from

Giemsa-stained blood smears. Error bars show the SD of three replicates from three independent experiments. **C)** *P. falciparum* viability time-course profiles in the presence of 49c (10 nM), chloroquine (CQ, 100 nM), and atovaquone (ATV, 10 nM). **D)** WT *P. falciparum* parasites were treated with 1 nM 49c for 6 or 40 hours. DMSO-treated control parasites re-invaded, whereas 49c-treated parasites were blocked at a fully mature schizont stage. The scale bars represent 2 µm. **E-F)** *P. falciparum* cultures were treated with 1 nM 49c at different time points before egress; ring and schizont stages were quantified. Compound 49c acts on its aspartic protease targets between 5 and 3 h prior to egress. In **(F),** the compound was washed-out 1 or 5 h before egress. **G)** Scheme of PfSUB1 and PfAMA1 maturation steps; the cleavage sites and the proteases responsible are indicated when known. The resulting products are shown and their molecular masses indicated. The pro-sequence of PfAMA1 is shown in pink. **H)** Immunoblots evaluating the processing of PfSUB1 upon DMSO/49c treatment. *P. falciparum* blood stage parasites were treated with 49c for 6 h. Parasites were allowed to egress for 15 or 30 min. The p54 precursor and the p47 active form of PfSUB1 are indicated with arrows. A very small proportion of the p54 PfSUB1 precursor was converted to the p47 active form when parasites were treated with 1 nM 49c (indicated with an asterisk). The lower 40-kDa band likely corresponds to a degradation product of PfSUB1. **I)** Electron micrograph of DMSO- or 49c-treated *P. falciparum* schizont stage parasites. WT parasites were used and fixed at the time of egress initiation or 30 min after. Black arrows highlight the RBC plasma membrane. Arrowheads label the PVM. Scale bars, 2 µm. **J)** WT parasites were treated with 1 nM 49c for 1, 5 or 40 hours before being mechanically released and allowed to invade. **K)** Immunoblots evaluating the processing of PfAMA1 upon DMSO/49c treatment. *P. falciparum* blood stage parasites were treated with 49c (1 nM) for 6 h. Parasites were allowed to egress for 15 or 30 min. The p83, p66, and p44 forms are indicated with arrows. A polyclonal anti-PfAMA1 serum recognizing

predominantly the precursor of PfAMA1 was used (*39*). In the right panel, a serum recognizing the p44 processed form was used (*40*).

Figure 2

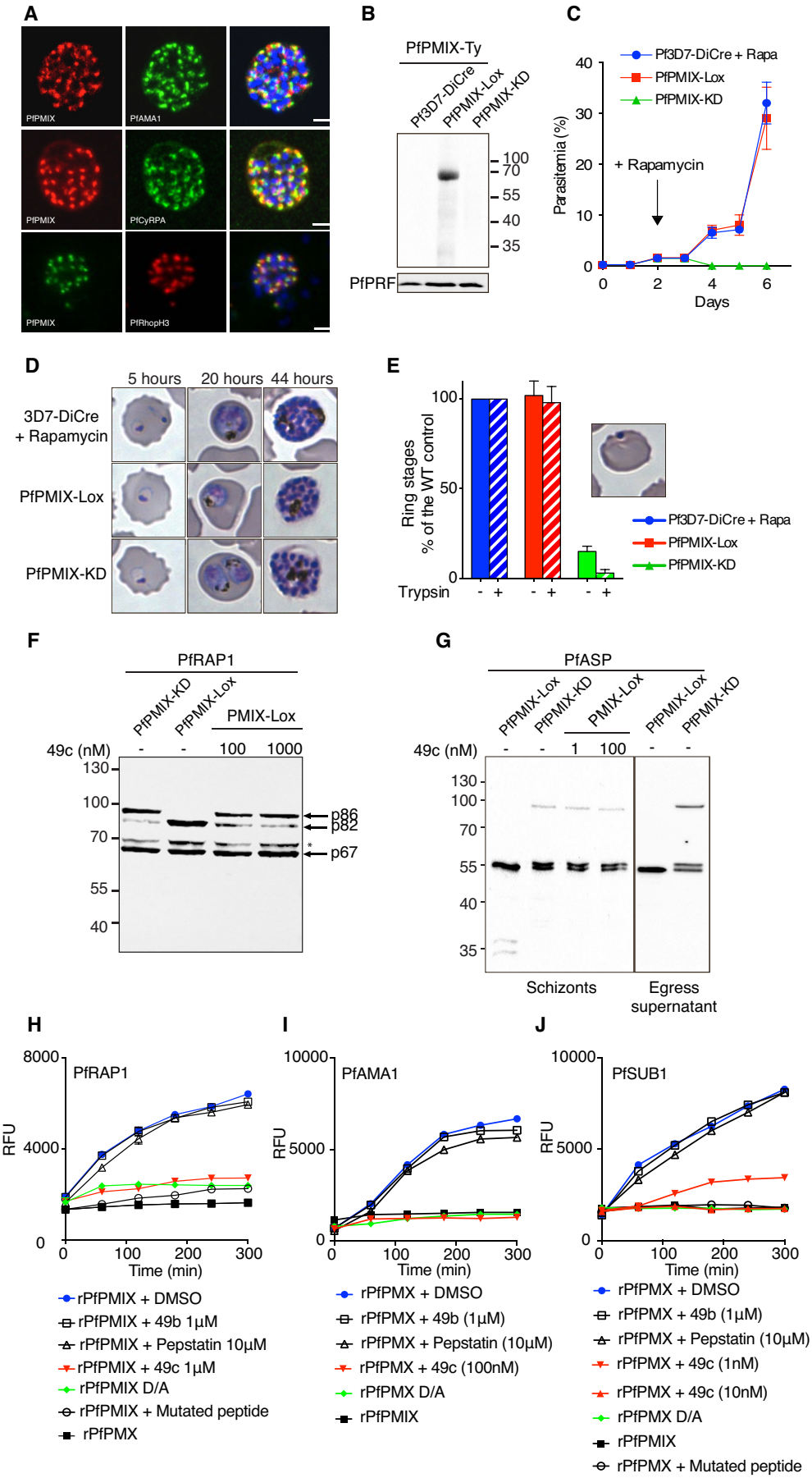
A
PfPMIX
PfAMA1
PfCyRPA
PfRhopH3
B
PfPMIX-Ty
Pf3D7-DiCre
PfPMIX-Lox
PfPMIX-KD
100
70
55
40
35
PfPRF
C
Pf3D7-DiCre + Rapa
PfPMIX-Lox
PfPMIX-KD
+ Rapamycin
Parasitemia (%)
Days
D
5 hours
20 hours
44 hours
3D7-DiCre + Rapamycin
PfPMIX-Lox
PfPMIX-KD
E
Ring stages % of the WT control
Trypsin
Pf3D7-DiCre + Rapa
PfPMIX-Lox
PfPMIX-KD
F
PfRAP1
PfPMIX-KD
PfPMIX-Lox
PMIX-Lox
49c (nM)
p86
p82
p67
G
PfASP
PfPMIX-Lox
PfPMIX-KD
PMIX-Lox
PfPMIX-Lox
PfPMIX-KD
49c (nM)
Schizonts
Egress supernatant
H
PfRAP1
RFU
Time (min)
rPfPMIX + DMSO
rPfPMIX + 49b 1µM
rPfPMIX + Pepstatin 10µM
rPfPMIX + 49c 1µM
rPfPMIX D/A
rPfPMIX + Mutated peptide
rPfPMX
I
PfAMA1
RFU
Time (min)
rPfPMX + DMSO
rPfPMX + 49b (1µM)
rPfPMX + Pepstatin (10µM)
rPfPMX + 49c (100nM)
rPfPMX D/A
rPfPMIX
J
PfSUB1
RFU
Time (min)
rPfPMX + DMSO
rPfPMX + 49b (1µM)
rPfPMX + Pepstatin (10µM)
rPfPMX + 49c (1nM)
rPfPMX + 49c (10nM)
rPfPMX D/A
rPfPMIX
rPfPMX + Mutated peptide

Figure 2. PfPMIX play a critical role in red blood cell invasion

A) IFAs showing the localisation of PfPMIX, relative to the microneme proteins PfAMA1, PfCyRPA and PfRhopH3. **B)** Immunoblot on schizont stage lysates from the 3D7-DiCre parental line, PfPMIX-Lox, and PfPMIX-KD after rapamycin treatment. Antibodies against PfPRF were used as a loading control. **C)** Representative replication curves. 3D7-DiCre parental line and PfPMIX-KD lines were treated with rapamycin at the ring stage, whereas the PfPMIX-Lox control was not. **D)** 3D7-DiCre and PfPMIX-Lox parasites were treated with DMSO/rapamycin at the ring stage, and intraerythrocytic development was monitored on Giemsa-stained blood smears 5, 20, and 44 hours post invasion. **E)** The invasion ability of 3D7-DiCre, PfPMIX-Lox, and PfPMIX-KD lines was quantified +/- trypsin treatment to remove non-invasive merozoites adherent on red blood cells. Cultures were treated with rapamycin at the ring stage and allowed to mature to the schizont stage. Schizonts were allowed to egress and re-invade for 4 hours before quantification. **F-G)** Immunoblots evaluating the processing of PfRAP1 and PfASP upon PfPMIX deletion and DMSO/49c treatment. PfPMIX-Lox parasites were treated at the ring stage with rapamycin or 1nM 49c for 10 hours. When fully mature, schizonts were collected. The p86, p82 and p64 forms of PfRAP1 are indicated with arrows. **H)** Typical progress curves showing cleavage *in vitro* of fluorogenic PfRAP1 substrate by recombinant rPfPMIX. 49b (1µM) and pepstatin (10µM) had no inhibitory effect on rPfPMIX catalytic activity at these concentrations, while a robust inhibition was observed in the presence of 1µM of 49c. rPfPMIX dead enzyme (first catalytic D mutated to A) and rPfPMPMX is used as control for the assay. rPfPMX cleavage of **I)** PfAMA1 and **J)** PfSUB1 peptides and its their inhibition in the presence of 49c (10 nM or 1 µM). The mutant PfSUB1 peptide was not cleaved by rPfPMX. Neither the rPfPMX dead enzyme nor rPfPMIX cleaved the PfSUB1 peptide. PfSUB1: DABCYL-G-SMLEVENDAE-G-EDANS, mutant PfSUB1: DABCYL-G-SMAAVENDAE-G-EDANS.

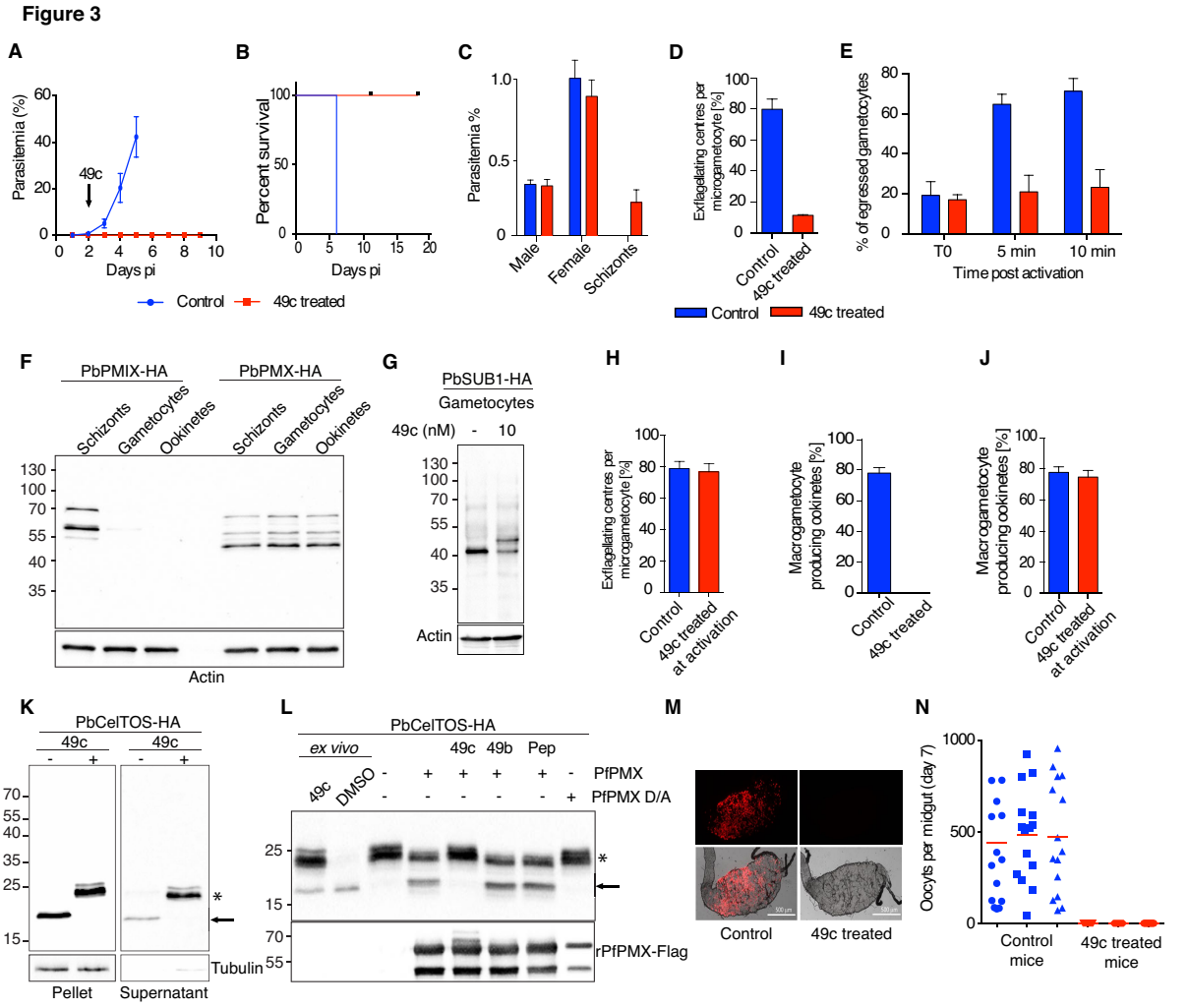

Fig 3. Compound 49c prevents malaria parasite transmission.

A-B) 49c cures malaria *in vivo*. Mice were infected with GFP-expressing *P. berghei* parasites at day 0. From day 2 to day 5, mice were injected i.p. daily with 100 mg/kg 49c. Parasitemia and survival curves are shown. n=5. **C)** Mice were infected with WT *P. berghei* parasites, and treated with 100 mg/kg 49c for two consecutive days. Parasitemia and gametocytemia were quantified. **D)** Gametocytes isolated from control and 49c-treated mice were activated *ex vivo*. The exflagellation rate at 20 min post-activation was calculated based on microscopic observations. Note that active flagellated gametes remained trapped in the host erythrocyte n=5. **E)** Gametocytes isolated from control and 49c-treated mice were activated *ex vivo*. Egress was quantified by FACS based on the presence of the erythrocyte membrane marker Ter-119 at the time of activation (T0), 5 and 10 min post-activation. n=4. **F)**

Immunoblot showing the expression of PbPMIX-HA and PbPMX-HA in blood stage schizonts, gametocytes and ookinetes. Actin was used as a loading control. **G)** Immunoblots evaluating the processing of PbSUB1 upon DMSO/49c treatment at the gametocyte stage. Mice infected with *P. berghei* expressing PbSUB1-HA were treated with 49c (100mg/kg for 48 hours) and sulfadiazine. Gametocytes were purified and processed for immunoblot analysis. **H)** Gametocytes isolated from untreated mice were activated *ex vivo* in the presence of 1 nM 49c/DMSO. The exflagellation rate at 20 min post-activation is shown. n=3. **I, J)** Gametocytes isolated from 49c-treated (**I**) or untreated (**J**) mice were activated *ex vivo* in the presence or absence of 1 nM 49c. Conversion to ookinetes was quantified 24 h post-activation. n=5. **K)** Immunoblots evaluating the processing of CelTOS and its secretion upon treatment with DMSO/49c. Gametocytes expressing a HA-tagged CelTOS were activated *ex vivo* ± 1nM 49c. Tubulin was used as loading control. **L)** Immunoblot showing the cleavage of PbCelTOS-HA immunoprecipitated from 49c-treated ookinetes in the presence of rPfPMX. Processing of PbCelTOS-HA is abrogated in the presence of 10nM 49c but not in the presence of 1µM 49b or 10µM pepstatin. rPfPMX D/A and PbCelTOS *ex vivo* samples and no enzyme are used as controls. The lower panel shows the presence of rPfPMX and rPfPMX D/A using Flag-tag antibodies. **M)** Female *An. stephensi* mosquitoes were fed on mice infected with mCherry-expressing *P. berghei* treated or not with 49c (ip. injection, 100 mg/kg, at 30 h prior blood feeding). At day 7 post feeding, from each mosquito cage (n=3) 15 mosquito midguts were dissected, fluorescent micrographs of the individual midguts were recorded, and the number of oocysts was determined. Representative pictures are shown. Scale bar 500 µm. **N)** The fluorescent oocysts from the individual microscopic pictures were counted. The graph shows the distribution of oocyst numbers per mosquito fed on the 3 control and 3 drug-treated mice.

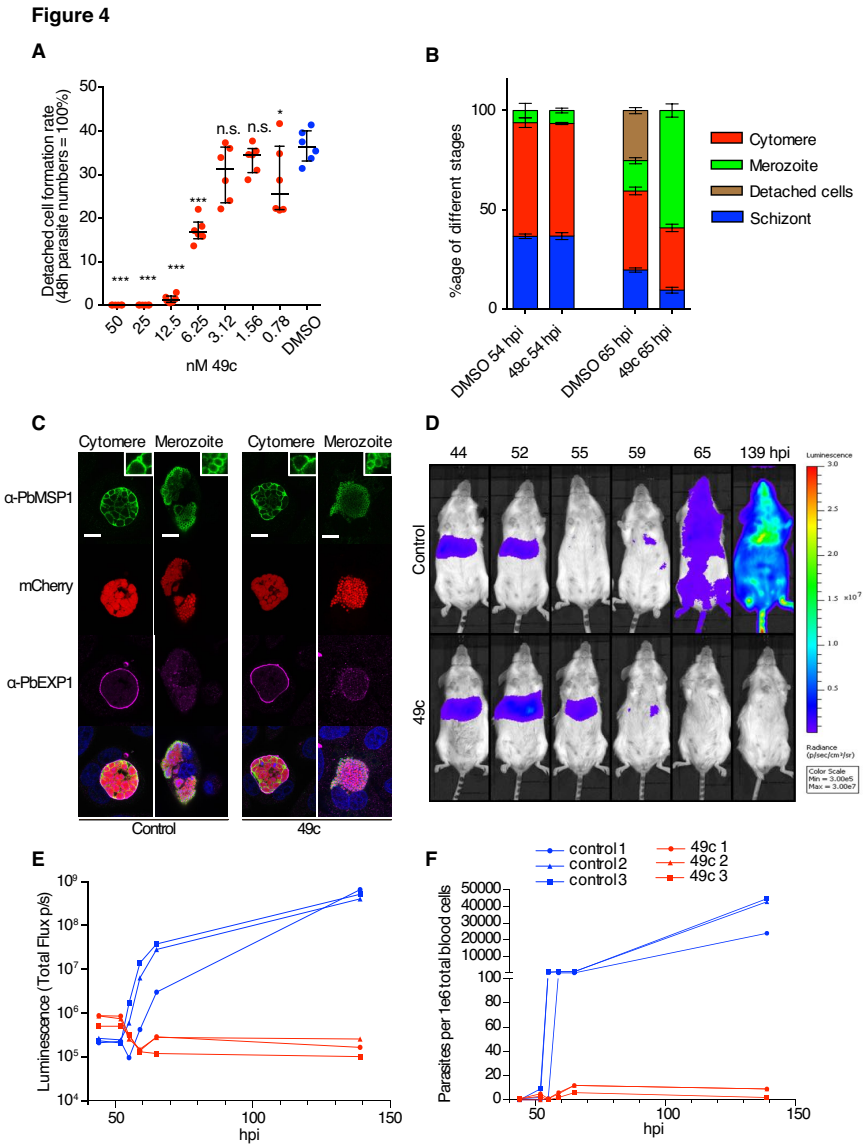

Fig 4. Compound 49c prevents hepatic merosomes formation.

A) The detached cell formation rate was reduced in 49c-treated *P. berghei*-infected HeLa cells in a dose-dependent manner. The results were statistically evaluated by a one-way ANOVA test with Dunnet's Multiple Comparisons (* $p \leq 0.05$, ** $p \leq 0.01$ *** $p \leq 0.001$, ns/not significant > 0.05). **B)** Distribution of the different hepatic stages by IFA of mCherry-expressing *P. berghei* in HeLa cells treated with 49c/DMSO 54 h and 65 h post infection. An anti-Msp1 antiserum was used to detect maturation of merozoites. Classification was done as reported before (*41*). **C)** Positive MSP1 staining of infected HeLa cells 65 h post infection

indicates normal merozoite development. At the cytomere stage, clear invaginations are visible and at the merozoite stage, individual merozoites are labelled with an MSP1 antibody. Exp1 is shown to visualize the PVM, (bar: 10μm, inserts are magnified 3x). **D)** Mice were infected by i.v. injection mCherry/Fluc expressing *P. berghei* sporozoites, and treated with 100 mg/kg 49c at 20 and 40 hpi (n=3). At indicated time points Rediject-D-Luciferin was administered and whole body luminescence detected using the *in vivo* imaging system (IVIS). In control mice, the luminescence signal from the liver disappears at 55 hours, the time when hepatic parasites egress. From 65 hpi blood stage parasites are detectable. In drug-treated mice the signal increased at 52 hpi and then remained longer in the liver (still present at 55 hpi) most likely because egress is blocked. **E)** The measured total flux (photons/second) in the head/chest region (blood stage parasites) of the mice in D is shown for the different time points. **F**) At each time point blood samples were analysed by FACS, detecting the mCherry signal of the parasite in 10^6 whole blood cells confirming the results obtained by bioluminescence imaging (**E**).

Supplementary Materials:

Materials and Methods

Figures S1-S5

Movies S1- S2

References 41-63